580.439 Course notes: Channels, selectivity, and permeation

Reading: Hille, chapters 9, 13, 14 and 16.

These notes will discuss ion permeation through channels using models that are closer to the structure of real channels than the thermodynamic models considered in the previous notes.

Properties of ion channels—where the thermodynamic models fail

The thermodynamic models derived in a previous set of notes assume a simple model for permeation, in which ions diffuse through homogeneous media under the influence of concentration gradients and gradients of electrical potential, as expressed by the Nernst-Planck equation:

$$I_i = u_i z_i F C_i \left[RT \frac{d \ln C_i}{dx} + z_i F \frac{dV}{dx} \right] \qquad (1)$$

where I_i is the flux of the i^{th} ion in the system in units of electrical current density (Amp/m^{2}s), u_i is the mobility of the ion, z_iF is the charge on a mole of ions, C_i is the concentration of the ion, RT is the gas constant times absolute temperature, and V is the electrical potential. The driving forces moving ions are the concentration gradient dC_i/dx and the gradient in electrical potential dV/dx. This form of the Nernst-Planck equation applies in one-dimensional systems (x), which is a reasonable assumption for ions crossing a membrane. Also the electrical convention for current flow has been adopted, in which current is positive when it flows from the positive to the negative side of the electrical potential gradient (in the negative x direction in this case).

An implicit assumption of Eqn. 1 is that the flows of ions through the system are independent of one other. Ion flows are linked together, of course, by the common electrical potential gradient V which they all share and help to generate. However, outside of this linkage, ion flows do not influence one another. Independence in this model arises simply because there are in the model no explicit mechanisms by which ions can influence one another. In real membranes, ions do not flow independently and they do not flow through diffuse homogeneous regimes of the type for which Eqn. 1 is appropriate. In real membranes, ions flow through specialized hydrophilic pores made by protein molecules called ion channels. These channels provide a variety of opportunities for interaction of ion flows. In these notes, more realistic and powerful models for ion flows through channels are considered.

Generally we are interested in a membrane of thickness d which separates two solutions, the inside and outside of a cell. The x axis in Eqn. 1 is perpendicular to the membrane and flows are assumed to occur only through the membrane parallel to x. Integration of Eqn. 1 through the membrane can be done with some assumptions, described in the previous notes, to give the following current-voltage relationship:

$$I_i = z_i F u_i RT \frac{C_i(inside) e^{z_i F \Delta V / RT} - C_i(outside)}{\int_0^d e^{z_i F V / RT} dx} \qquad (2)$$

The current density is expressed in terms of the concentration difference across the membrane (C_i(outside) minus C_i(inside)) and the membrane potential difference $\Delta V=V_{inside}-V_{outside}$. The integral in the denominator cannot be evaluated without additional assumptions, such as the constant field assumption. For the present purposes, however, the details of the denominator term, which is a function only of the membrane potential, are not important. The model of Eqn. 2 fails to adequately represent several important features of currents through real ion channels.

1. **Saturation:** the simplest departure from the predictions of Eqn. 2 derives from the fact that any membrane contains only a finite number of channels. Each channel can conduct ions at a certain maximum rate, so the flux through a membrane must saturate when all the channels present are conducting at their maximum rates. The model of Eqn. 2, of course, predicts that flux is linearly proportional to concentration of ions, regardless of concentration. Examples of saturating ion fluxes as the concentration increases are given in Hille (pp. 302-309 and 363-367). Saturation is easily accounted for by models in which ions must compete for a finite number of transport sites in the membrane.

2. **Independence**: an important property of thermodynamic fluxes is that the unidirectional fluxes in the system should have a fixed ratio. By unidirectional flux is meant ions moving in one direction only through the membrane. The net flux, I_i in Eqns. 1 and 2, is the sum of an inward and an outward unidirectional flux. Unidirectional flux can be measured by making a fraction of the ions on one side of the membrane radioactive and measuring the appearance of radioactivity on the opposite side. Eqn. 2 is clearly the difference of two unidirectional fluxes which can be written separately as follows:

$$I_{i\,Outward} = z_i F u_i RT \frac{C_i(inside) e^{z_i F \Delta V/RT}}{\int_0^d e^{z_i FV/RT} dx} \qquad \text{and} \qquad I_{i\,Inward} = -z_i F u_i RT \frac{C_i(outside)}{\int_0^d e^{z_i FV/RT} dx} \quad (3)$$

where the outward flux is taken to be the flux that depends on the ionic concentration inside the cell $C_i(inside)$ and vice versa. The ratio of these two fluxes (ignoring the sign) is the flux ratio

$$\frac{I_{i\,Outward}}{I_{i\,Inward}} = \frac{C_i(inside) e^{z_i F \Delta V/RT}}{C_i(outside)} = e^{-z_i F E_i/RT} e^{z_i F \Delta V/RT} = e^{z_i F(\Delta V - E_i)/RT} \quad (4)$$

A plot of the natural log of the flux ratio $\ln[I_{i\,Outward}/I_{i\,Inward}]$ versus the electrochemical driving potential (ΔV-E_i) should be a straight line with slope z_iF/RT, which is 1/26 /mV for a univalent cation like potassium (z_i=1). For potassium channels in particular, the deviation from this prediction is significant. Usually the slope of such plots is 2-4 times larger in potassium channels than the prediction of Eqn. 4 (see Fig. 7, p. 375 of Hille). The interpretation of this finding is that the potassium channel contains a long narrow pore which can contain more than one potassium ion. In order for ions to move through the channel, they must do so cooperatively, in a single file fashion, since it is unlikely that ions can pass one another in the narrow pore. Thus the process of either influx or efflux of an ion involves the cooperative movement of 2-4 ions, and this ensemble carries a charge 2-4 times the unit charge, explaining the steeper slope.

The evidence from flux ratios, along with the anomalous mole-fraction effect discussed later in these notes, provides clear evidence that ions must interact directly with one another in channels. This generally requires a more complex model, one in which two or more ions can be in the channel simultaneously and interact with one another.

3. **Rectification**: the current-voltage relationship is a plot of the current through a channel as a function of the voltage across the membrane, for fixed ion concentrations. Figure 1 shows examples of current-voltage relationships computed from a model for ion permeation developed below. Most channels have approximately linear current-voltage relationships, like the one marked λ=0.5. However, channels can pass current more easily in the inward direction (inward rectifying, λ=1 in Fig. 1) or in the outward direction (outward rectifying, λ=0 in Fig. 1). This property of channels is called rectification.

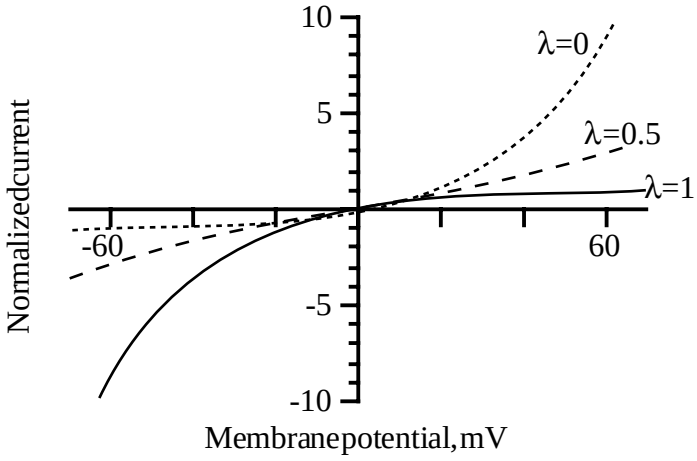

Fig. 1 Current-voltage relationships for the single barrier model (see Eqn. 32) with zero equilibrium potential. λ is the fraction of the transmembrane potential seen at the barrier peak. Membrane potential is positive inside the cell and current is positive outward, as usual. Current is plotted in normalized form, as $I/(const)\exp(-G/RT)z\,FA$, see Eqn. 32.

There are several known mechanisms for rectification. In the early literature, voltage dependent gating was sometimes considered to be rectification (as in the delayed rectifier channel). However, for the present discussion, rectification refers only to nonlinearities in the current voltage relationships of open channels. One source of rectification was discussed in the previous notes on thermodynamic models. The inward and outward currents in Eqn. 2 will be different in the ratio $C(outside)/C(inside)$ which gives a rectification. This effect is likely to be significant for calcium channels in real cells, since the concentration ratio of calcium across the membrane is large ($\approx 10^4$). Concentration-dependence can account for only certain types of rectification, however (e.g. outward rectification in potassium channels and inward rectification in calcium and sodium channels, see Eqn. 35 and Fig. 12 of the notes on thermodynamic models) and does not explain all observed cases of rectification.

A second source of rectification is block of a channel by an impermeant ion. For example, magnesium ions block some potassium channels (so-called inward rectifiers) from the inside of the cell. When the membrane potential becomes depolarized enough to drive Mg^{++} currents in the outward direction, the ions enter the channel from the inside of the cell, but cannot pass all the way through the channel. They apparently bind tightly enough to the channel that K^+ ions are unable to permeate, preventing outward flows of potassium, and giving this channel a strong inward rectification (see Hille pp. 481-484). A similar

Mg^{++} block is observed in the opposite direction (from outside) in certain glutamate receptor channels (see Hille, pp. 167-169).

4. **Selectivity:** the most striking property of ion channels is their selectivity for different ions. Channels are classed as potassium, sodium, calcium, or chloride channels, based on the ions that can permeate. Often, channels are able to select between chemically almost identical ions (e.g. sodium and potassium) and this ability to pass selectively one kind of ion current is the basis for electrical signaling in nerve membranes.

Selectivity is usually quantified experimentally as the ratio of the permeabilities of pairs of ions based on the thermodynamic theory developed previously. Consider the case of two monovalent ions. Suppose that it is possible to measure the membrane potential in a situation like Fig. 2 where only the two ions *A* and *B* are permeable through the membrane and suppose also that there is only one active channel in the membrane. Based on the thermodynamic theory developed in the previous notes, the potential ΔV across the membrane when there is zero net current through the membrane (the reversal potential) can be written as

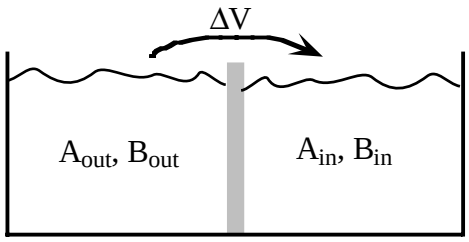

Fig. 2 A membrane separates two solutions containing the indicated concentrations of ions *A* and *B*.

$$\Delta V = \frac{RT}{F}\ln\frac{P_A A_{out} + P_B B_{out}}{P_A A_{in} + P_B B_{in}} = \frac{RT}{F}\ln\frac{\frac{P_A}{P_B}A_{out} + B_{out}}{\frac{P_A}{P_B}A_{in} + B_{in}} \qquad (5)$$

where P_A and P_B are the permeabilities of the ion through the channel. Equation 5 allows determination of the permeability ratio P_A/P_B from the membrane potential ΔV and the concentrations. This equation was derived in the previous notes in terms of the mobility u_i. The permeability is a generalization of mobility which takes into account the partitioning of the ion between the solution and the membrane. Permeability ratios determined in this way for the squid giant axon sodium channel are given in table 1 (from Hille, p. 351). The sodium channel selects for sodium over calcium and potassium by about a factor of 10, using this measure. By the same measure, potassium and calcium channels are even more selective.

Table 1
Permeability ratio P_X/P_{Na} for squid giant axon Na channel

X	P_X/P_{Na}
H^+	>2
Li^+	1.1
Na^+	1.0
Ca^{++}	0.1
K^+	0.08
Rb^+	0.025
Cs^+	0.016

Accounting for channel selectivity requires consideration of the details of ion permeation through channels (see Hille, Chapters 13 and 14). At present, the portions of the protein molecule that are responsible for the selectivity of several types of channels are known (in that mutating the amino acids at those locations changes channel selectivity), but detailed

theories to explain the selectivity have not appeared. Some aspects of ion selectivity can be accounted for by charge (e.g. anions cannot flow through channels with fixed negative charges in the pore) and size (e.g. molecules that are larger than the pore cannot squeeze through). But neither of these effects can account for the relative selectivity of sodium, potassium and calcium channels. For example, the sodium ion Na^+ is smaller than the potassium ion K^+ and has the same charge, but potassium channels discriminate against sodium by a factor of between 10 and 100. A simple theory which points the way to accounting for selectivity is discussed below.

5. **Gating:** the most important property of ion channels for neural modeling is their gating, meaning the ability of the channel to open and close in response to changes in membrane potential or the presence of neurotransmitters. However, in these notes, we consider only the properties of open channels. Gating is discussed later.

Structure of ion channels

Ion channels are formed by a variety of protein molecules. However, the channels most important for neural modeling have structures like those sketched in Fig. 3. The top half of Fig. 3 shows the subunits that make up a nicotinic acetylcholine receptor channel (NAChR, left) and a voltage gated potassium channel (right). Each subunit is a single protein molecule. The membrane is indicated by the shaded areas. The molecule is shown as a string, corresponding to the string of amino acids that make up the protein. Ion channels consist of components that are outside the membrane, drawn as lines, and transmembrane domains, drawn as cylinders (indicated *M1 – M4* and *S1 – S6*). The transmembrane domains are α helices consisting largely of amino acids with hydrophobic side chains which stabilize these parts of the molecule in the membrane. The full NAChR consists of five such subunits, i.e. five of the molecules drawn at upper left. The subunits are not identical but are very similar and are named α - ε. They usually are combined in the ratio $\alpha_2\beta\gamma\delta$ or $\alpha_2\beta\varepsilon\delta$ and are arranged in a pentameric structure like the one shown at lower left in Fig. 2. The pore (*P*) is formed jointly by all five subunits; evidence from mutations at various sites in the subunit molecules suggests that the *M2* transmembrane domains form the walls of the pore. Essentially, replacing negatively charged amino acid residues in the *M2* segment (but not the other three segments) with neutral or positively charged residues reduces the conductivity of the channel (see Hille, pp. 423-427). The inhibitory receptor channels activated by glycine and GABA have structures similar to that of the NAChR.

Potassium channels are formed by a combination of four subunits like the one drawn at right in Fig. 3. In the case of the potassium channel, the pore is made up of the *S5, S6*, and *P* segments jointly, in a structure that will be described in more detail below. Voltage gated sodium and calcium channels have a structure similar to the potassium channels, except that the four subunits making up a channel are combined into one molecule. Some potassium channels (mostly inward rectifier channels) are made of subunits containing only the pore forming elements *S5, S6* and *P*.

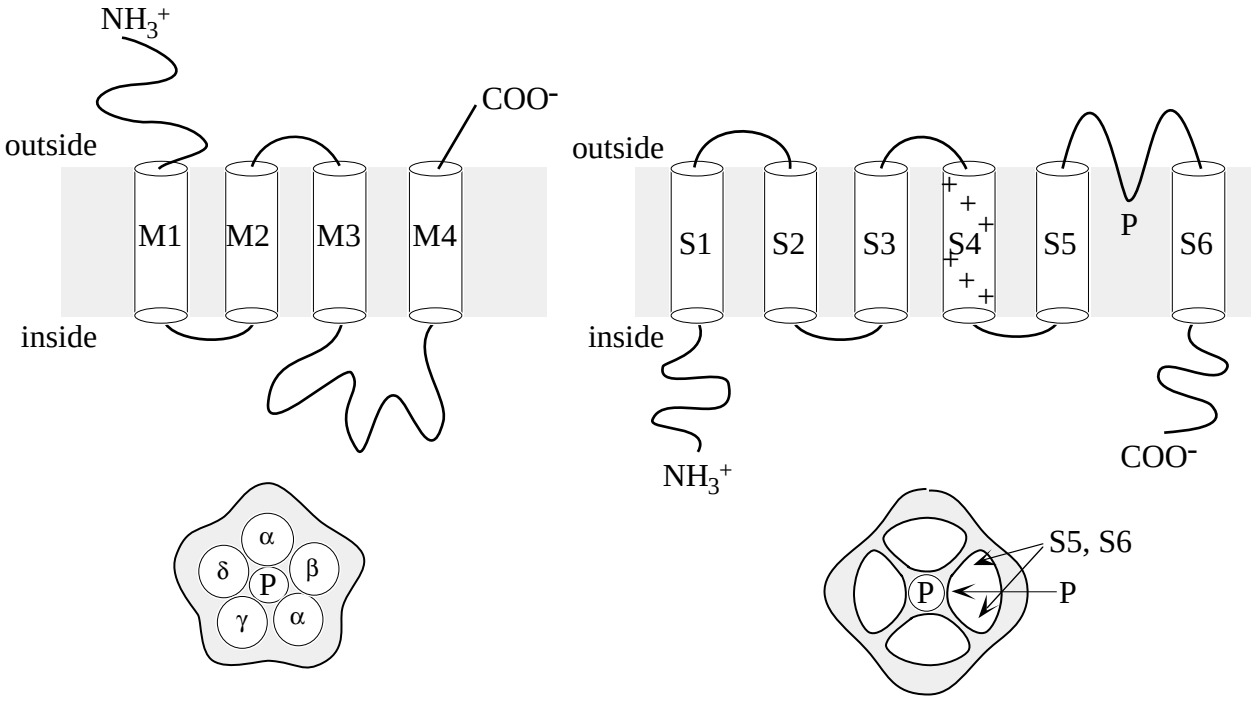

Fig. 3 Top row: molecular structure of the subunits of the nicotinic acetylcholine receptor channel (left) and the voltage gated potassium channel (right). The shaded area is the membrane; cylinders are transmembrane segments consisting of α helices. Below: structure of the channel looking perpendicular to the membrane. *P* is the pore, formed by *M2* segments of the NAChR and by the *P, S5,* and *S6* segments of the potassium channel. α, β, γ, and δ are different subunits of the NAChR, all with similar structures based on the plan above.

For the present purposes, it is the structure of the pore which is of most interest. In the NAChr, the pore-forming elements (the *M2* helices) contain amino acids with negatively charged side chains at three positions along the helix. These forms three rings of negative charges, one just at the outer surface of the membrane, a second just at the inner surface of the membrane, and a third within the membrane (see also Fig. 2, p. 425 of Hille). These data plus electron micrographic images of the NAChr suggest that this channel looks roughly like Fig. 4 (see also pp. 242-244 of Hille). The rings of negative charge probably provide binding sites that stafbilize cations in the pore, thereby providing a hydrophilic channel through which ions can move. This channel is selective for cations with little or no discrimination among ions; the permeability ratios are 1.4/1.1/1.0/0.9/0.3 for the ions $Cs^+/K^+/Na^+/Li^+/Ca^{++}$. These permeabilities, plus those measured for a variety of organic and inorganic cations suggest that the pore is fairly large, with an inner diameter of about 6 Å. There is an additional ring of polar amino-acids, at the

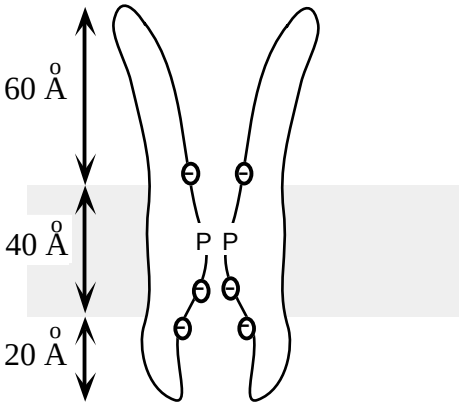

Fig. 4 Sketch of the likely structure of the NAchR in cross section. Horizontal shaded rectangle is the membrane. Dimensions are from electron micrographic data. Three rings of charge are located in the approximate positions shown by the circled – signs. *P* marks the locus of an additional ring of polar amino acids which participate in channel selectivity. The channel contains a gate at the narrowest portion of the pore.

position marked *P* in Fig. 4, that also participates in determining selectivity.

The KcsA channel

The best information about the structure of ion channels comes from one molecule whose structure has been determined from X-ray crystallography. Figure 5 shows a sketch of this potassium channel, the KcsA channel of a bacterium. The material in this section is all taken from a paper describing the channel's structure (Doyle et al., 1998) and from a recent review of potassium channels which discusses the implications of the KcsA structure for voltage gated potassium channels in general (Yellen, 1999). The KcsA channel is a simplified version of the potassium channel sketched in Fig. 3; it has only the *S5, P,* and *S6* domains. It lacks voltage-dependent gating (which is contributed by the *S4* domain) but is otherwise very similar to voltage-gated potassium channels. The sequence of amino acids in the *S5, P, S6* domains is highly conserved across different channels and the structure of the pore of the KcsA channel is thought to be similar to that of voltage gated channels.

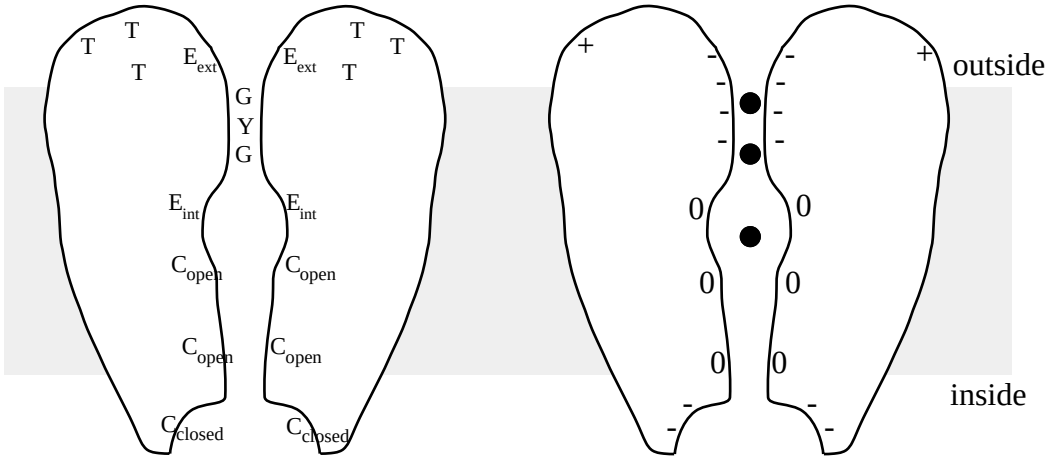

Fig. 5 Schematic of the molecular structure of the bacterial KcsA potassium channel, modified from Doyle et al., 1998. Approximate locations of various chemically identified sites, inferred from data on the Shaker K^+ channel, are shown at left: *T* binding sites for agitoxin 2 or charybdotoxin acting from outside the cell; E_{ext} binding site for agitoxin or TEA acting from outside the cell; E_{int} binding site for TEA acting from inside the cell; C_{open} sites which can be reached only when the channel's gate is open; C_{closed} sites which can be reached with the gate closed; *GYG* location of the glycine, tyrosine, glycine residues which have been shown to be the selectivity filter. At right, the + and - symbols show the locations of amino acid residues on the surface of the channel with net positive or negative charge at physiological pH; the 0s show the locations of hydrophobic residues lining the pore. The black circles are high probability locations of potassium ions within the channel.

The overall structure of the KcsA channel is set by the *S5* and *S6* segments, which are arranged to form a cone with its wide part (base) at the outside of the membrane and its narrow part (tip) at the inside of the membrane. The pore is constructed partly by one of these segments, which forms the inside half of the pore, and by the *P* segments, which form the outside half of the pore. For full details about the molecular structure of the channel, see the original papers.

A satisfying aspect of the structure determined for the KcsA channel is that it is consistent with a variety of previous indirect evidence as to the location in the channel molecule of various amino acids. These experiments were done in the so-called Shaker channel, a voltage-

gated potassium channel from drosophila. Because the amino-acid sequence of the Shaker *S5*, *P*, and *S6* segments show high homology to the corresponding regions in KcsA, it is possible to relate a mutation made at one site in Shaker to the location of that site determined in KcsA. Those data are summarized in the left half of Fig. 5. First, binding sites are found in the expected places on the channel. Binding sites for toxins and blockers that act from outside the cell (*T*, and E_{ext}) are found on the outside of the channel and binding sites for blockers acting from the inside (E_{int}) are found on the inside of the channel. More important, binding sites that can be reached with the voltage gate of the Shaker channel closed (C_{closed}) are found on the inside surface of the molecule and binding sites that can only be reached with the channel's gate open (E_{int} and C_{closed}) are found within the pore of the channel.

The KcsA channel does not show voltage gating, but the Shaker channel does. The data on binding sites summarized above suggests that the voltage gate in the Shaker channel must be at the narrow point in the channel near its inside surface (between C_{closed} and C_{open}). The nature of this gate is unknown, but one might speculate that the gate operates by bringing together the inside ends of the *S5* and *S6* domains to block the channel pore. Although the KcsA channel is not voltage gated, its pore is closed by low pH. At the pH used to determine the structure of the channel, it is likely that the pore was closed. Thus the structure shown in Fig. 5 may correspond to a closed channel. In that case, one can speculate that the open channel would show a wider opening at its inner end.

Three amino acids (glycine, tyrosine, glycine) near the intramembrane tip of the *P* domain are known to convey the ion selectivity of potassium channels, in the sense that mutations of these amino acids degrade the selectivity of the channel. These amino acids were found in the positions marked *GYG* in Fig. 4. These residues form the *selectivity filter* of the channel. As expected, the selectivity filter occupies the narrowest portion of the channel. The nature of the filter is somewhat clarified by the structural data. The pore in the region of the selectivity filter is formed by the protein backbone and not the side chains of the amino acids. Thus ions sitting at this point in the channel would interact with the negative ends of the electrical dipoles that are formed by the oxygen atoms of the protein's peptide bonds. Because there is a *GYG* sequence in each of the four subunits forming the channel, the pore at the selectivity filter will have several rings of four oxygen dipoles surrounding the pore. Presumably it is the electrostatic interaction of potassium ions with these oxygen rings that conveys selectivity on the channel.

The tyrosine residues of the selectivity filter have a substantial side chain containing an aromatic ring. This ring is directed away from the pore. Doyle and colleagues suggest that the interactions of this ring with other parts of the molecule provide a mechanical stabilization of the pore in the region of the selectivity filter. It may turn out that the stiffness of this mechanical structure is important to selectivity. That is, with an ion in the pore in this region, the oxygens will be pulled into the pore by the electrostatic attraction of the positively charged ion and the degree of movement of the pore wall, as governed by the stiffness of the interactions of the tyrosine side chains with the rest of the molecule, may be important in setting the properties of selectivity.

The final property shown in Fig. 5 is the location of surface charge on the molecule. The + and – signs show the locations of amino acids with net charge at physiological pH. Notice that

the entrances to the pore and the outside half of the pore have a net negative charge, as would be expected for a cation channel. As was discussed for the NAChr channel, these negative charges will have the effect of stabilizing cations in the pore and excluding anions from the pore. For the charges near the entrances to the pore, the fixed charges will attract cations to the pore (discussed in the next section).

The black circles in the right half of Fig. 5 show the locations of electron densities in the structural determination that correspond to potassium ions. Apparently, potassium ions spend more time at these sites and the sites might be considered to be binding sites for potassium in the pore. Two of these sites are associated with the selectivity filter and the third is in the middle of the large part of the pore in the center of the membrane. The size of the pore in the inside of the membrane is such that a potassium ion could sit here in association with substantial water, i.e. the ion could be fully hydrated at this position. Roux and MacKinnon (1999) have analyzed the electrostatic interactions between an ion at this site and the charges and dipoles in the protein. They conclude that this site would be a favorable one for a potassium ion, mainly because of the electrostatic effects of dipoles formed by the α helices of the *P* segments of the subunits (not shown in Fig. 5) which are directed at this site.

A surprising aspect of the KcsA channel structure is that the inside half of the pore is lined by hydrophobic residues (0s in Fig. 5), which are uncharged, have no dipoles, and cannot form hydrogen or other electrostatic bonds. This half of the pore should be relatively hydrophobic and therefore should not be a favorable site for ions. However, as discussed in the previous paragraph, the presence of water molecules in this part of the pore and electrostatic effects not shown in the drawing in Fig. 5 do stabilize ions at this site.

Effects of surface charge on ion concentrations and potentials near channels

The structure of the KcsA channel shown in Fig. 5 has net negative charge at the inner and outer surfaces of the channel. Such surface charge is important for two reasons. First, it modifies the concentrations of ions near the entrances to the channel, increasing the cation concentration and decreasing the anion concentration. These concentration changes contribute to channel selectivity and may also increase the conductivity of the channel. Second, the potentials produced by the surface charge affect channel gating. In this section, the Poisson-Boltzman theory of surface potentials is presented to demonstrate some properties of these effects.

Consider the simplified situation shown in Fig. 6. A surface has a charge Q (coul/m^2) distributed uniformly on it and faces a solution containing bulk concentrations C_i (moles/m^3) of several ions. For simplicity, only one cation C^+ and one anion C^- are shown. Qualitatively, the negative surface charge produces a negative potential V in the solution, which attracts positive charge, increasing C^+ and decreasing C^-, as drawn. The problem is assumed to be one-dimensional, i.e. concentrations and

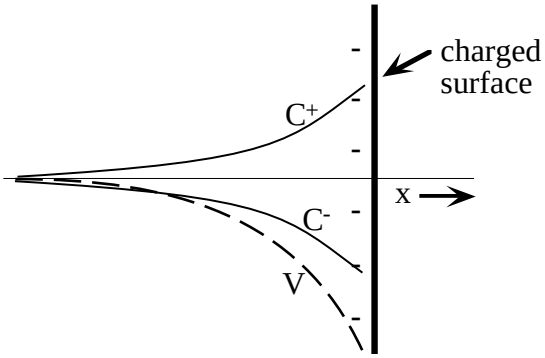

Fig. 6 Concentrations of a cation C^+ and an anion C^- in a solution near a surface with fixed negative charge Q (coul/m^2). V is the potential near the surface.

potentials vary only with *x*, perpendicular to the surface.

In the Poisson-Boltzman model, the ions are assumed to be in equilibrium in the vicinity of the membrane. Writing the equilibrium in terms of the molar free energy used in the previous notes on thermodynamics gives the following condition for each of the ions in the system:

$$\text{constant} = \mu_i(x) = \mu_i^0 + RT\ln C_i(x) + z_i F V(x) \tag{6}$$

That is, the ion is at equilibrium in the solution if its molar free energy μ_i is constant at all values of *x*. The constants can be determined by applying the conditions that the concentration is $C_i(-\infty)$ in the bulk solution and the electrical potential is zero there, $V(-\infty)=0$, i.e.

$$\text{constant} - \mu_i^0 = RT\ln C_i(-\infty) \tag{7}$$

$$\text{so that} \quad RT\ln C_i(-\infty) = RT\ln C_i(x) + z_i F V(x) \tag{8}$$

$$\text{or} \quad C_i(x) = C_i(-\infty)e^{-z_i FV(x)/RT} \tag{9}$$

Equation 9 is a Boltzman distribution, in which the concentration of the ion is exponentially related to the potential the ion sees.

To solve for the electrical potential, consider that $V(x)$ is related to the charge density $q(x)$ (in coul/m^3) by Poisson's equation:

$$\frac{d^2V}{dx^2} = -\frac{q(x)}{\varepsilon\varepsilon_0} \tag{10}$$

where ε is the dielectric constant (80 for aqueous solutions) and ε_0 is 0.9 x 10^{-11} coul/volt-m. The charge density in solution is the sum of the charges carried by various ions:

$$q(x) = \sum_i z_i F C_i(x) \tag{11}$$

where the sum is taken over all ions in the solution. Combining Eqns. 9, 10, and 11

$$\frac{d^2V}{dx^2} = -\frac{1}{\varepsilon\varepsilon_0}\sum_i z_i F C_i(-\infty)e^{-z_i FV(x)/RT} \tag{12}$$

This non-linear differential equation cannot be solved in closed form. To get an idea of the form of the solution, use the approximation $e^x \approx 1+x$, which holds for $x<<1$. Equation 12 then becomes

$$\frac{d^2V}{dx^2} \approx -\frac{1}{\varepsilon\varepsilon_0}\left[\sum_i z_i F C_i(-\infty) - \sum_i z_i F C_i(-\infty)\frac{z_i FV(x)}{RT}\right] \tag{13}$$

This approximation will be true in the limit of potentials $V(x)$ small compared to RT/z_iF. The first sum in the brackets in Eqn. 13 is zero because the net ionic charge in bulk solution must be zero (equal concentration of cations and anions). The differential equation then takes the form

$$\frac{d^2V}{dx^2} \approx \frac{F^2\sum_i z_i^2 C_i(-\infty)}{\varepsilon\varepsilon_0 RT} V(x) = \frac{1}{L^2} V(x) \quad \text{where} \quad L = \sqrt{\frac{\varepsilon\varepsilon_0 RT}{F^2\sum_i z_i^2 C_i(-\infty)}} \tag{14}$$

The quantity L is called the Debye length. It is the length over which the charge imbalances and the potential sketched in Fig. 6 will extend into the solution.

The solution to Eqn. 14 is a sum of exponentials

$$V(x) = Ae^{x/L} + Be^{-x/L} \tag{15}$$

As was assumed in Eqn. 7, the potential V should be 0 in the bulk solution far from the membrane ($x \to -\infty$), so B=0. To determine A , apply the condition that the net excess of charge in the solution should equal the charge on the surface, so that the total charge across the whole region will sum to 0. The charge density (coul/m^3) is given by Eqn. 11 plus the contribution Q from the surface charge, so

$$0 = Q + \int_{-\infty}^{0} q(x)\,dx = Q + \int_{-\infty}^{0} \sum_i z_i F C_i(-\infty) e^{-z_i FV(x)/RT}\,dx \tag{16}$$

$$\approx Q + \int_{-\infty}^{0} \sum_i z_i F C_i(-\infty)\left[1 - \frac{z_i FV(x)}{RT}\right] dx \tag{17}$$

$$= Q + \int_{-\infty}^{0} \sum_i z_i F C_i(-\infty)\,dx - \int_{-\infty}^{0} \sum_i \frac{z_i^2 F^2 C_i(-\infty)}{RT} Ae^{x/L}\,dx \tag{18}$$

Equation 16 expresses the condition that the charge in solution per unit area of membrane surface should equal the negative of the surface charge. In Eqn. 17, the same approximation was made as in Eqn. 13. In Eqn. 18, the solution (Eqn. 15) for $V(x)$ has been substituted. The integrand of the first integral in Eqn. 18 is identically zero from the bulk electroneutrality condition used above (Eqn. 13). Evaluating the second integral and solving for A gives

$$A = \frac{QL}{\varepsilon\varepsilon_0} \quad \text{so} \quad V(x) = \frac{QL}{\varepsilon\varepsilon_0} e^{x/L} \quad \text{and} \quad \mathrm{V}(0) = \frac{QL}{\varepsilon\varepsilon_0} \tag{19}$$

The important results are Eqns. 14 and 19. For biological solutions, L is usually about 10 Å, so the effects of surface charge are felt only locally near the membrane surface. Because L is so small, it is not feasible with current technology to directly measure the effects of surface charge. The Debye length increases as the solutions become more dilute, i.e. when there are fewer ions in solution. A longer Debye length means both that the effect of surface charge extend further into solution but also that the potential at the surface $V(0)$ is larger. An important point is

that divalent ions have a much larger effect on the Debye length (and surface potential) than univalent ions, because of the z^2 term in Eqn. 14. This can cause problems in experiments if the concentration of divalent charges is changed, because the surface charge and potential will change.

Estimates of surface charge are inexact, but values between 1 charge per 100 Å^2 and 1 charge per 400 Å^2 are often stated. With these charges and a Debye length of 10 Å, the potential at the surface from Eqn. 19 is between 55 and 220 mV. These values are larger than RT/F (26 mV), so the approximation made in deriving the expressions above (Eqns. 13 and 17) does not hold. Using the exact expression (see Question 1), the range is 48-112 mV. With these potentials, Eqn. 9 predicts that the concentration of univalent cations (Na^+, etc.) should be increased near the surface by between 6.3 and 74 times, and the concentration of divalent cations (Ca^{++}, etc.) should be increased by between 40 and 5500 times. The concentrations of anions will be decreased by similar amounts. Clearly surface potentials produced by fixed charges on the channel can substantially affect the concentrations of ions at the entrance to the channel pore.

The existence of a surface potential implies that the potential across the membrane itself is not the same as the potential in the bulk medium. This situation is illustrated in Fig. 7, which shows a membrane with a transmembrane potential ΔV, measured between the bulk solutions and two surface potentials, V_{OS} and V_{IS}, each given by Eqn. 19. The surface potentials are not necessarily equal because the density of surface charge and the Debye lengths in the solutions on the two sides of the membrane are not necessarily equal. As a result, the actual potential seen by an ion channel in the membrane is not ΔV, but $\Delta V - V_{OS} + V_{IS}$ (ΔV_{actual} in Fig. 7). The voltage-dependent gates of a channel are likely to be affected by the potential modified by the surface charge (ΔV_{actual}), not by ΔV itself, so that changes in surface charge are likely to produce changes in the apparent voltage sensitivity of gating, as defined in terms of bulk solution potentials. Hille (pp. 457-470) discusses the evidence for this effect of surface charges.

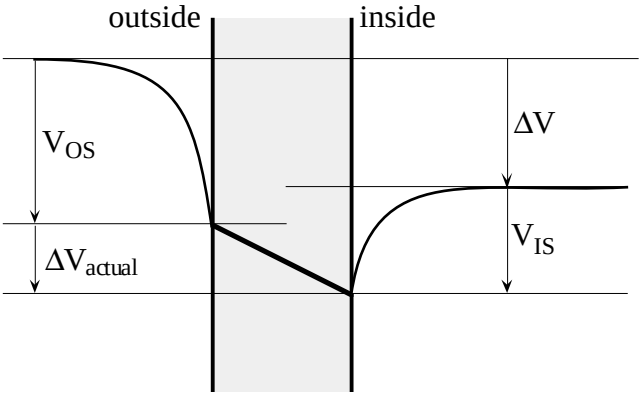

Fig. 7 Membrane with a transmembrane potential ΔV measured in the bulk solutions. Because of surface potentials V_{OS} and V_{IS}, the actual transmembrane potential ΔV_{actual} differs from that measured in the bulk solutions.

Question 1: Work out the solution to Eqn. 12 for a special case that does not require making the linear approximation of Eqn. 13.

1. Assume that the solution contains only one cation at concentration $C^+(-\infty)$ and charge z^+ and one anion at concentration $C^-(-\infty)$ and charge z^-. Assume that $C^+(-\infty) = C^-(-\infty)$ and that $z^+ = -z^-$ (charge electroneutrality in the bulk solution). Show that Eqn. 12 can be written as follows:

$$\frac{d^2V}{dx^2} = \frac{1}{L^2}\frac{RT}{zF}\sinh\left(\frac{zFV(x)}{RT}\right) \tag{20}$$

Write an expression for L in this case.

2. Show that, with the assumption that $V(-\infty)=dV(-\infty)/dx=0$, Eqn. 20 can be integrated once to give

$$\frac{dV}{dx} = \frac{2}{L}\frac{RT}{zF}\sinh\left(\frac{zFV(x)}{2RT}\right) \tag{21}$$

(Hint: do this by substitution; be careful of the 2s here!) Eqn. 21 can be integrated again to write a very messy formula for $V(x)$. Work this out if you are interested.

3. Apply the condition used in writing Eqn. 16, that Q should equal the negative of the integral of the net charge in solution from $x=-\infty$ to 0, to derive the following expression for the relationship between the surface charge and the potential at the surface $V(0)$:

$$Q = \frac{2\varepsilon\varepsilon_0}{L}\frac{RT}{zF}\sinh\left(\frac{zFV(0)}{2RT}\right) \tag{22}$$

(Hint: Eqns. 10, 11, and 21 will be useful here). For this special case, Eqn. 22 is the exact version of the approximation of Eqn. 19. Show that Eqn. 22 reduces to Eqn. 19 if $V(0)<<RT/zF$.

Eisenman model for ion selectivity

Ion channels exhibit striking selectivity among chemically similar ions (such as the alkali metal cations Li^+, Na^+, K^+, Rb^+, and Cs^+). This selectivity must arise from the subtleties of interactions between ions and the parts of the channel molecule forming the walls of the selectivity filter. A general theory for selectivity has not emerged, but a model proposed by Eisenman (1960) provides an idea as to the nature of selectivity. In studies of glass ion-selective electrodes, Eisenman observed that, although there are 120 possible sequences for the relative permeabilities of the five ions Li^+ through Cs^+, only 11 of these are commonly observed. He accounted for these 11 by an equilibrium binding model which proposes that the selectivity derives from the interaction of two effects: the energy required to remove an ion from its hydration shell in solution (Table 2) and the electrostatic energy of binding of the ion to a site in the channel. Thus, it is assumed that the ion must lose its hydration shell in order to enter the channel; it is also assumed that the ion is stabilized in the channel by electrostatic interactions with a charged binding site. The first assumption is supported by data on the size of the pores in channels (reviewed by Hille, pp. 355-361), which suggest that ions must be fully or partially dehydrated in order to pass through the channel.

Table 2

	crystal radii	hydration energy
Li^+	0.6 Å	-131 kCal/mole
Na^+	0.95	-105
K^+	1.33	-85
Rb^+	1.48	-79
Cs^+	1.69	-71

The relative affinity of a channel for various ions can be estimated by comparing the free energy change that ions undergo from being hydrated in solution to being bound to a site in the channel. That is, consider the process of moving from solution into the channel as having two-steps: in the first step, the ion loses its hydration shell; in the second step, it binds to an oppositely charged site in the channel. The ion's free energy change is then

$$\Delta G_{total} = \Delta G_{\text{dehydration}} + \Delta G_{\text{bind to site}} \tag{23}$$

The channel will be selective for the ion with the most negative ΔG_{total}, i.e. the ion for which dehydration and binding to the channel is most energetically favorable. The dehydration energies are the negatives of the hydration energies in Table 2. The hydration energies are large and negative, which means that being hydrated in solution is an energetically very favorable state for an ion. The hydration energy is smallest in magnitude for Cs^+, meaning that Cs^+ is easiest to dehydrate and therefore would be easiest to move into a channel if dehydration were the only step.

As a technical note, the energies in Table 2 are actually enthalpies, where enthalpy H is defined as $H=U+PV=G+TS$. Thus, enthalpy differs from free energy G by a term involving entropy. For dilute solutions, the enthalpy change should be very similar to the change in total energy U, because $\Delta(PV)$ should be small; moreover, the calculation of $\Delta G_{bind\ to\ site}$ described below is also accurate as a calculation of ΔU. However, Eisenman uses "free energy" to refer to these calculations, and his notation has been maintained here.

For the energy of binding to the site, Eisenman used the negative of the work required to remove the ion from the site and carry it to an infinite distance in a vacuum. Assuming that this work is done against the Coulombic force of attraction of the two charges,

$$\Delta G_{\text{bind to site}} = -\int_{R_0+r_0}^{\infty} (const)\,\frac{q_{ion}\,q_{site}}{r^2}\,dr \tag{24}$$

where q_{site} and q_{ion} are the charges on the site in the channel and on the ion and r is the distance between the binding site and the ion. The force between two such charges when separated by a distance r is $(\text{const})q_{ion}q_{site}/r^2$ from Coulomb's law. That force integrated through distance is the work done on the ion to separate it from the site. Eisenman assumed that the site is spherical with radius R_0 and that the ion has radius r_0, so that the charges are separated by distance R_0+r_0 when the ion is bound to the site. Evaluating the integral in Eqn. 24 gives

$$\Delta G_{\text{bind to site}} = -(const)\,\frac{q_{ion}\,q_{site}}{R_0 + r_0} \tag{25}$$

The value of the constants $(const)q_{ion}q_{site}$ is 332 in the units Eisenman used (energies in kCal/mole, distances in Å). The free energy change for binding (Eqn. 23) can now be computed from Eqn. 23, using Eqn. 25 and the hydration energies in Table 2. The r_0 values, i.e. the ionic radii, are taken from the first column in Table 2. The radius of the site R_0 is a variable. In the Eisenman model, R_0 is the parameter that controls ion selectivity.

Figure 8 shows the values of ΔG_{total} from Eqn. 23, as values relative to Cs^+, i.e. as ΔG_{total}(ion) - ΔG_{total}(Cs), plotted versus R_0, the radius of the binding site. The most negative (or least positive) plot at each value of R_0 is the ion that has the energetically most favorable binding to the channel for that value of binding site size. The plot shows that, as the binding site radius changes, the sequence of channel-binding preference changes. For large binding sites (R_0 greater than about 1.75 Å), the binding sequence Cs>Rb>K>Na>Li holds. For large binding sites, the $\Delta G_{bind\ to\ site}$ (Eqn. 25) is approximately constant, because the ionic radii are small compared to the binding site size; that is, the denominator of Eqn. 25 is dominated by R_0 and not by r_0. Thus the relative binding is controlled by the dehydration energy, and the ion with the least hydration energy (Cs) is favored. By contrast, for small binding sites (R_0 less than about 0.95 Å), the sequence Na>Li>K>Rb>Cs holds. For small binding sites, the effect of ion radius r_0 on the binding energy (Eqn. 25) is large and $\Delta G_{bind\ to\ site}$ dominates the overall free energy change. In this case, the ion with the smallest radius r_0 will be most favored. If the graph in Fig. 8 were extended to smaller binding sites, the curve for Li^+ would cross the curve for Na^+, and the final permeability sequence, Li>Na>K>Rb>Cs would be seen. This sequence is completely determined by ionic radius.

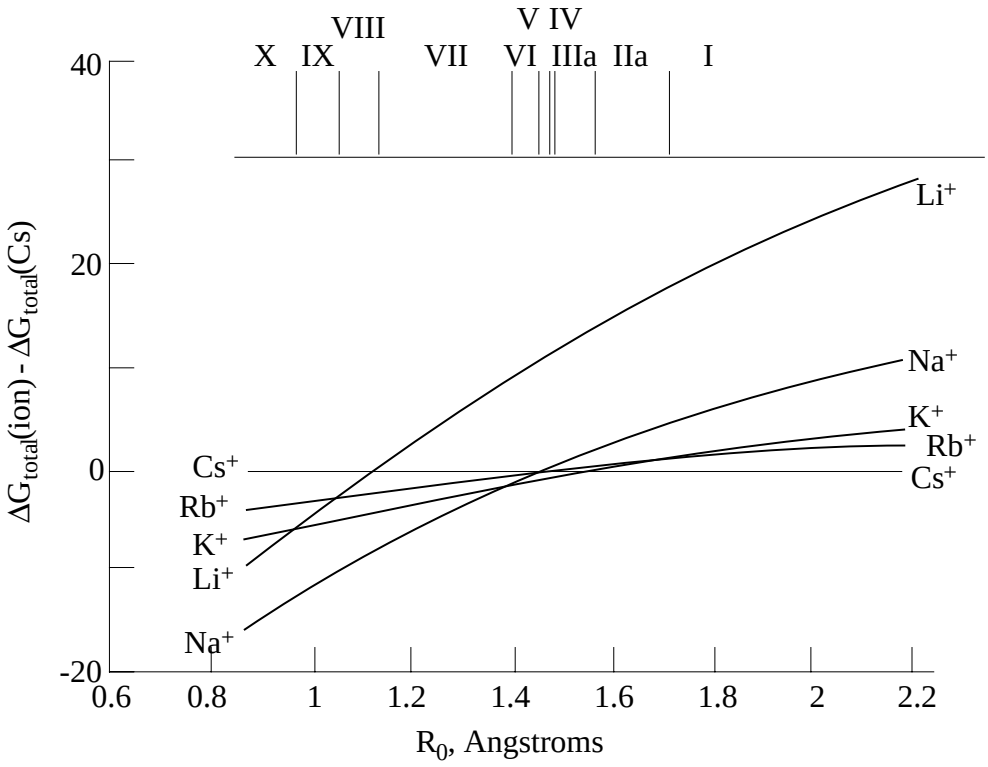

Fig. 8 Plot of free energy change for binding to an anionic site versus the site radius for the Eisenman model. Energies are show relative to the energy for Cs. Eisenman sequences are shown above.

The scale at the top of the graph identifies the range of R_0 over which each of 1 Eisenman sequences is observed (the 11th sequence occurs for smaller R_0 values). For the model used in Fig. 8, these sequences are as follows:

I.	Cs > Rb > K > Na > Li	VI.	K > Na > Rb > Cs > Li
IIa.	Cs > K > Rb > Na > Li	VII.	Na > K > Rb > Cs > Li
IIIa.	K > Cs > Rb > Na > Li	VIII.	Na > K > Rb > Li > Cs

IV. K > Rb > Cs > Na > Li
V. K > Rb > Na > Cs > Li
IX. Na > K > Li > Rb > Cs
X. Na > Li > K > Rb > Cs
XI. Li > Na > K > Rb > Cs

Note that a slightly different list of Eisenman sequences is given in Hille (p. 289). These are the sequences which result if it is assumed that the binding sites in the channel are close together and dense, in which case six cations bind to six adjacent sites (the strong field strength assumption). This assumption does not change the basic theory, but does change some of the curves plotted in Fig. 8 and results in a slightly different order of crossing of the curves for sequences II and III. Eisenman explored several other assumptions and showed that each led to small changes in the eleven sequences listed above.

The fact that the Eisenman theory predicts common ion selectivity sequences suggests that the simple ideas on which the theory is based may capture the essential ingredients of channel selectivity.

Permeation—the rate theory model

The structure of ion channels reviewed in a previous section suggests that ion permeation might be modeled as a so-called barrier hopping process. Using the NAChr as an example, the channel's pore contains a sequence of fixed charge sites. As suggested by the Eisenman theory, it is likely that such sites are necessary to provide the energy to break the hydrogen bonds maintaining the ion in solution, i.e. to provide the energy to dehydrate the ion so it can enter the channel. With this assumption, permeation of an ion through a channel can be thought of as a stepwise process in which the ion moves from binding site to binding site within the ion's pore. At each binding site, the electrostatic attraction of the ion for the site provides an energy well in which the ion can sit in an energetically favorable situation. In moving between binding sites, the ion must acquire enough thermal or other energy to overcome the electrostatic attraction to the sites. A cartoon of this model is shown in Fig. 9. Although the structure of the KcsA channel does not contain obvious binding sites, the data do suggest that ions preferentially occupy three positions in the pore (black circles in Fig. 5). Thus permeation through this channel may take the form of rapid movements from solution to the high probability locations and rapid movements among these locations, essentially a sequence of hops through the pore.

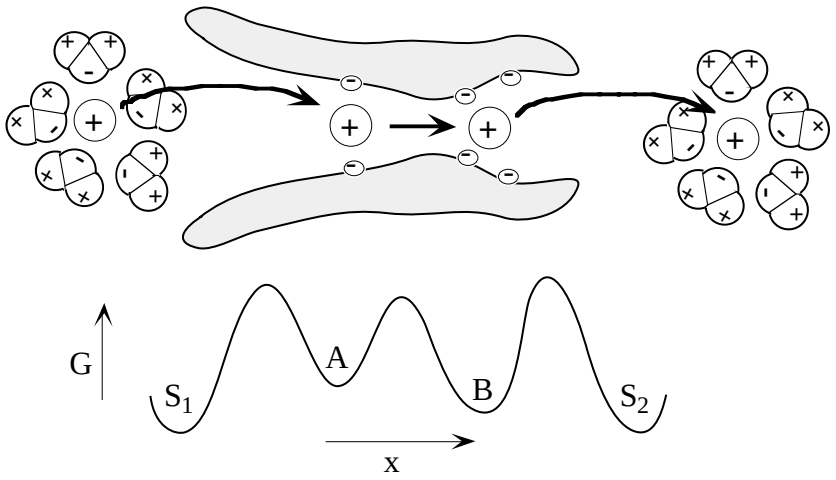

Fig. 9 Top: Cartoon view (not to scale!) of a cation moving from hydrated in solution to bound to sites in a channel to hydrated in solution again. Bottom: energy barrier model for the permeation process. S_1 and S_2 represent the ion hydrated in solution on the two sides of the membrane, *A* and *B* represent the ion bound to sites in the channel.

The physical transition through a sequence of sites in the pore has been modeled as a transition over a series of energy barriers, as drawn in the bottom part of Fig. 9. This plot shows a hypothetical picture of the energy an ion has versus its position in the channel. The potential wells occur at sites S_1 and S_2, which represent the ion hydrated in solution on the two sides of the membrane, and at sites *A* and *B* which represent the ion bound to one of two sites in the channel. The energy peaks separating the wells represent the amount of energy the ion must acquire to pass over the barrier. In the model, the process of permeating through a channel is assumed to be equivalent to transiting through the energy barrier system. (In actuality the barriers should not be considered to represent physical interactions of the ion with the channel as implied by Fig. 9; the problems with this approach will be discussed later.)

The process of passing over a barrier is modeled using Eyring rate theory. Consider the single barrier shown in Fig. 10. The barrier height is *G* (units of Joules/mole) and there is a difference in energy level between the two potential wells of *G**. Permeation across the barrier takes place with the rate constants k_1 and k_{-1} (units m/s). Thus the unidirectional fluxes across the barrier are given by

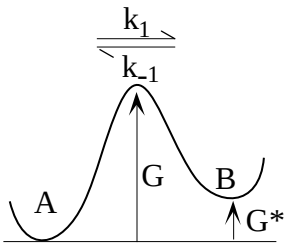

Fig. 10 Single barrier system.

$$J_{A\to B} = k_1 A \quad \text{and} \quad J_{B\to A} = k_{-1} B \tag{26}$$

A and *B* are the concentrations (units of moles/m^3) in the two energy wells. The net flux is the difference between the two unidirectional fluxes. The rate constants are exponential functions of barrier height as follows:

$$k_1 = (const)e^{-G/RT} \quad \text{and} \quad k_{-1} = (const)e^{-(G-G^*)/RT} \tag{27}$$

These expressions for rate constants are based on the assumption that, in order for an ion to pass across a barrier, it must acquire at least as much thermal energy as the barrier height. The probability of an ion having that much or more thermal energy is the negative exponential of the barrier height (Boltzman distribution), so the concentration of ions available to pass from *A* to *B* is $Ae^{-G/RT}$ and the concentration of ions available to pass from *B* to *A* is $Be^{-(G-G^*)/RT}$. The constant in Eqn. 27 is the rate at which ions with sufficient thermal energy will cross the barrier. In the Eyring theory applied to ion channels, this is $\kappa dkT/h$, where κ is a geometrical constant, *d* is the distance between sites (units of m), *kT* is the thermal energy per degree of freedom of a single particle, and *h* is Planck's constant. $kT/h = 6.1\text{x}10^{12}$ /s. The net flux is then the difference between the two unidirectional fluxes in Eqn. 26.

$$J = (const)Ae^{-G/RT} - (const)Be^{-(G-G^*)/RT} \tag{28}$$

$$= (const)e^{-G/RT}(A - Be^{G^*/RT}) \tag{29}$$

This equation resembles the equations resulting from integrating the Nernst-Planck equation (e.g. Eqn. 2) by having a term that depends on the difference in the concentrations on the two sides of the membrane.

In order to apply the barrier model to ion channels, membrane potential must be added to the barrier system. This is done by modifying the energy levels in the system by an electrical

potential function. Figure 11 shows the barrier system of Fig. 10 with electrical potential *V* added. The difference in the potential wells *G** has been removed to simplify the drawing; the system in Fig. 11 would be appropriate if site *A* were on one side of a membrane and site *B* were on the other, so that the potential wells have the same energy, in the absence of membrane potentials (*G**=0). *V* is the transmembrane potential, so the energy at site *B* is increased by *zFV*. The energy at the barrier peak is increased by λ*zFV*, where λ is the fraction of the membrane potential seen when the ion is at the location of the barrier. Figure 11 is drawn as if the constant field assumption were being made, i.e. the electrical potential increases linearly with distance through the model. However, this is done only for convenience in drawing the picture. The only assumption that is actually made is that the fraction of membrane potential seen at the barrier is λ. Substituting the barrier heights from Fig. 11 into Eqns. 26 and 27 gives

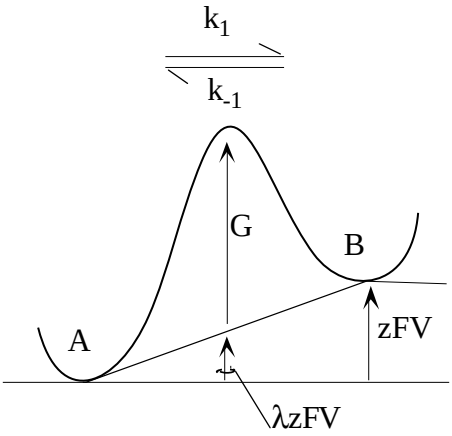

Fig. 11 The single barrier model of Fig. 10 modified by the addition of a transmembrane electrical potential *V*. *V* is defined as potential inside the cell (on the right) minus potential outside the cell (on the left), as usual. λ is the fraction of *V* seen by the ion at the barrier peak.

$$J = (const)\, e^{-(G+\lambda zFV)/RT}\,(A - Be^{zFV/RT}) \qquad (30)$$

Eqn. 30 now has an identical dependence on concentration as in the Nernst-Planck result (Eqn. 2).

The model of Eqn. 30 can be used to explain how different types of rectification can arise in an ion channel. The equilibrium potential of the ion is $E = RT/zF \ln(A/B)$, where *A* is assumed to the concentration of the ion outside the membrane and *B* is the concentration inside. Equation 30 can be rewritten by factoring an *A* out of the parentheses and substituting using the equilibrium potential to give

$$J = (const)\, A\, e^{-(G+\lambda zFV)/RT}\,(1 - e^{zF(V-E)/RT}) \qquad (31)$$

Equation 31 describes the flux through the membrane, which is positive in the +*x* direction, into the cell in Fig. 11. Using the convention that current is positive in the outward direction, and multiplying by *zF* to convert flux to current density, the current-voltage relationship for this model becomes:

$$I = (const)\, zF\, A\, e^{-G/RT}\, e^{-\lambda zFV/RT}\,(e^{zF(V-E)/RT} - 1) \qquad (32)$$

Equation 32 is plotted in Fig. 1 for three values of λ. Notice that when λ=0, i.e. when the barrier is at the outside of the membrane, the channel is outwardly rectifying, whereas when λ=1, i.e. with the barrier at the inside of the membrane, the channel is inwardly rectifying. The channel produces approximately linear current-voltage relationships for a barrier in the middle of the membrane. Thus a barrier model can explain a variety of channel rectification properties by simply varying the fraction of the membrane potential seen at the barrier height. In terms of permeation through a real channel, rectification depends on how much the membrane potential affects the rate limiting step in the permeation process.

Barrier models have been successful in explaining a number of complex properties of ion channels and have been very influential in guiding thinking about ion permeation (see the next section and Hille, chapters 14 and 15 for more examples). However the barrier model may not be an accurate description of the actual permeation process. For one thing, the assumptions made in defining the rate constants are incorrect. The constant term $\kappa dkt/h$ is appropriate for the situation originally considered by Eyring, a reaction occurring in a gas phase where the molecules are relatively widely spaced. In a liquid phase, molecules are closely spaced and an ion interacts constantly with water molecules to produce a frictional effect that makes the appropriate rate constant about 4 orders of magnitude smaller than $\kappa dkT/h$. This difference makes it impossible to quantitatively predict the properties of permeation (such as the conductance of a channel) from first principles using a barrier model. The correctness of the idea of permeation as a sequence of steps through the membrane remains to be determined. The results from the KcsA channel certainly imply that ions occupy a series of finite, high probability states as they pass through the channel. In this sense, the barrier model might be considered to be a way to describe such a series of discrete steps, as a curve fit to a kinetic scheme which approximates permeation. However, the geometry of the barrier model should not be considered to be an accurate reflection of the actual physical interactions of an ion with the channel. These issues are considered in more detail in the commentaries by Levitt (1999), Nonner (1999), and Miller (1999).

Question 2: Write an equation for the condition under which the flux through the single barrier system of Fig. 10 and Eqn. 29 is zero. Consider this to be the condition for equilibrium between states *A* and *B*. Reconcile this definition of equilibrium with equilibrium as defined in terms of the electrochemical potential in Eqn. 13 of the Notes on Thermodynamics. Is the flux in Eqn. 32 also consistent with equilibrium thermodynamics?

The two-barrier, one-site model

The barrier model in Fig. 12 allows a number of insights into channel permeation to be derived. This model consists of two barriers, with a single potential well in the membrane. The barriers and rate constants are defined in the figure, along with the electrical potential. Note that it has been assumed that the electrical potential divides equally among the three sites; this assumption is made for simplicity in the derivations and does not affect the final outcome in any important way. The rate constants are defined as follows:

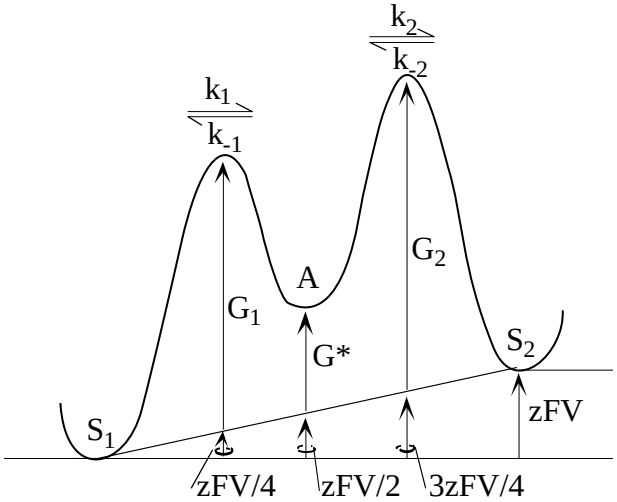

Fig. 12 Two barrier, one site model.

$$k_1 = \alpha e^{-(G_1 + zFV/4)/RT} = \alpha e^{-h_1 - v/4} \qquad k_2 = \beta e^{-(G_2 + 3zFV/4 - G^* - zFV/2)/RT} = \beta e^{-h_2 + h^* - v/4}$$
$$k_{-1} = \beta e^{-(G_1 + zFV/4 - G^* - zFV/2)/RT} = \beta e^{-h_1 + h^* + v/4} \qquad k_{-2} = \alpha e^{-(G_2 + 3zFV/4 - zFV)/RT} = \alpha e^{-h_2 + v/4} \tag{33}$$

To reduce the complexity of the expressions, the energies have been expressed in dimensionless units, as multiples of RT, so that $h_i = G_i/\mathrm{RT}$ and $v = zFV/RT$. The constants α and β are the rate expressions as above, except that α and β are different because k_1 and k_{-2} are second order rate constants whereas k_{-1} and k_2 are first order rate constants (see below).

The fluxes over the barriers are given by the following equations:

$$J_1 = k_1 S_1 X - k_{-1} A \tag{34}$$

$$J_2 = k_2 A - k_{-2} S_2 X \tag{35}$$

$$Q = A + X \tag{36}$$

The variable X is the concentration of unbound channel, i.e. channels without an ion in their binding site; A is the concentration of channel with an ion bound. The unidirectional flux from S_1 to A (Eqn. 34) is proportional to the rate constant k_1 times the product of S_1 and X, to express the fact that an ion can only enter an unbound channel. The unidirectional flux from S_2 (Eqn. 35) has a similar form. Equation 36 expresses the fact that (for the first time in these notes) there is a finite number Q of channels and that only one ion can occupy each channel.

An additional assumption that is necessary in order to solve for flux in this model is that the system is in steady state. This means that all quantities are constant in time. In particular, the concentration of channel containing an ion (A) is constant. If A is to be constant, then $J_1=J_2$, that is the flux into the channel from solution 1 must equal the flux out of the channel into solution 2. With this additional assumption, Eqns. 34-36 are three equation in three unknowns (J , A, and X). They can be solved to give the following expression for flux:

$$J = \frac{k_1 k_2 S_1 - k_{-1} k_{-2} S_2}{k_1 S_1 + k_{-1} + k_{-2} S_2 + k_2} Q \tag{37}$$

$$= \alpha\beta Q \frac{e^{h^*} e^{-(h_1+h_2)} e^{-v/2}\left[S_1 - S_2 e^{v}\right]}{e^{h^*}\beta\left[e^{-(h_1-v/4)} + e^{-(h_2+v/4)}\right] + \alpha\left[e^{-(h_1+v/4)} S_1 + e^{-(h_2-v/4)} S_2\right]} \tag{38}$$

Question 3: Notice that Eqn. 38 retains an important feature of the integrated Nernst-Planck equation (Eqn. 2), which is the term involving S_1 and S_2 in the brackets in the numerator. Show that flux is zero when the ion is at thermodynamic equilibrium across the membrane.

Three inferences about flux through barrier systems can be drawn from Eqns. 37 and 38:

1. Because of the assumption of a finite number of channels, these expressions are saturating, that is, the flux has a limited maximum (saturating) value as concentration S_1 and S_2 increase. This is most easily seen from Eqn. 37 and derives from the S_1 and S_2 terms in the denominator.

2. At low concentrations, where $S_1 << k_{-1}/k_1$ and $S_2 << k_2/k_{-2}$, the terms dependent on concentration in the denominator can be ignored. In this condition, Eqn. 38 can be approximated as follows:

$$J \approx \alpha Q \frac{e^{-(h_1+h_2)}}{e^{-(h_1-v/4)}+e^{-(h_2+v/4)}} e^{-v/2}\left[S_1 - S_2 e^{v}\right] \tag{39}$$

Notice that the dependence of the flux on h^* disappears from the equation. That is, at low concentrations where most of the channels are not occupied by an ion, the flux does not depend on the depth of the energy well at the binding site in the channel (h^*). In addition, the form of this equation is the same as Eqn. 2, from the Nernst-Planck theory, except for the form of the dependence on membrane potential. In particular, notice that the model obeys the flux ratio test for independence in this situation. Finally, notice that the larger of the two barriers will control the flux in this situation. That is, if (for example) $h_1 > h_2$ so that $e^{-h_1} << e^{-h_2}$ then

$$J \approx \alpha Q\, e^{-h_1}\, e^{-v/4}\left[S_1 - S_2 e^{v}\right] \tag{40}$$

and the flux depends only on the first barrier. That is, in the low concentration range, the flux is controlled by the highest barrier in the system.

3. At high concentrations, where $S_1 >> k_{-1}/k_1$ and $S_2 >> k_2/k_{-2}$, the constant terms in the denominator can be ignored and the flux equation becomes

$$J \approx \beta Q\, e^{h^*}\, e^{-(h_1+h_2)}\, e^{-v/2}\, \frac{S_1 - S_2 e^{v}}{e^{-(h_1+v/4)} S_1 + e^{-(h_2-v/4)} S_2} \tag{41}$$

Now the binding site h^* is important and flux varies directly as e^{h^*}. Note that this means that a channel that binds an ion tightly (more negative value of h^*) will have a low flux. This occurs when the ion binds so tightly to the channel that it cannot leave the channel once it is inside. Flux also depends on the energy peaks in the high concentration limit.

An alternative model—PNP

The alternative theoretical approaches to modeling channel permeation vary from potentially very accurate but entirely computational approaches (molecular dynamics), in which the detailed motions of every atom making up a channel are modeled, to a model called PNP (for Poisson-Nernst-Planck). There is a series of models in between molecular dynamics and PNP involving successive degrees of simplification, and therefore potential inaccuracy. These models are summarized quite nicely by Levitt (1999). All of these models differ from the barrier models in that they assume that ions move through channels by a continuous process (as opposed to a hopping process) which is limited by frictional effects.

In the PNP model, the Nernst-Planck equation is used to represent the flow of ions under the influence of concentration gradients, electric fields, and (sometimes) an added chemical potential gradient $d\mu/dx$ which is used to represent inhomogeneities in the interior of a channel that are not captured by the electric field effects. In its one-dimensional form, this equation is as follows:

$$J = -D\left[\frac{dC}{dx} + \frac{C}{RT}\frac{d}{dx}(\mu + zFV)\right] \tag{42}$$

Equation 42 is identical to the Nernst-Planck equation used previously in these notes (Eqn. 1), except for the $d\mu/dx$ term mentioned previously. Also, the diffusion coefficient D is used instead of the identical uRT. The use of the Nernst-Planck equation expresses the assumption that the motion of an ion in a pore is not a barrier-jumping process, i.e. a process consisting of a finite sequence of jumps through the channel, but rather a continuous diffusion process characterized by frictional interactions with water or the channel wall.

The electric field dV/dx within the channel is assumed to be the field created by all the charges and dipoles in the channel molecule along with the ions present in the channel. It is computed from Poisson's equation:

$$\frac{d}{dx}\left[\varepsilon(x)\frac{dV}{dx}\right] = \frac{1}{\varepsilon_0}\sum_k \rho_k \tag{43}$$

which takes into account the fact that the dielectric constant ε can change with position in the channel. The right hand side of Eqn. 43 is the sum of all the charges in the channel and in the channel wall. These include fixed charges on amino acids in the protein, dipoles in the protein, and ions in the channel.

Equations 42 and 43 give a flavor of the PNP models for channel permeation. The advocates of these and more complex models prefer them because they are based on a more realistic model of ion movement (diffusion versus barrier hopping) and because they offer the possibility of representing the channel's actual structure through the $\mu(x)$ and $\rho_k(x)$ functions. There are problems, especially with the one-dimensional version of PNP (see Miller, 1999). For the purposes of these notes, a severe problem is that closed-form solutions of Eqns. 42 and 43 cannot be obtained, so that properties of channel permeation, like rectification, saturation, etc. can be discovered only through simulations. This is even more true for the most accurate of the methods, molecular dynamics, which requires large computing resources to obtain results for very short times, less then the time taken for an ion to permeate the channel. Nevertheless, the availability of the structure of the KcsA channel has allowed very useful molecular dynamic studies of the potassium channel pore. For examples of applications of molecular dynamics simulations to this problem, see Åqvist and Luzhkov (2000) and Guidoni et al. (2000). The paper of Åqvist and Luzhkov, for example, shows that hopping between sites is actually not a bad model for the mechanics of permeation of K^+ through the KcsA channel, as seen in molecular dynamics calculations.

References

Åqvist, J. and Luzhkov, V. (2000) Ion permeation mechanism of the potassium channel. *Nature* 404:881-884.

Doyle, D.A., Morais Cabral, J., Pfuetzner, R.A., Kuo, A., Gulbis, J.M., Cohen, S.L., Chait, B.T., and MacKinnon, R. (1998) The structure of the potassium channel: Molecular basis of K^+ conduction and selectivity. *Science* 280:69-77.

Eisenman, G. (1960) On the elementary atomic origin of equilibrium ionic specificity. In: *Symposium on Membrane Transport and Metabolism*, A. Kleinzeller and A. Kotyk (eds.), Academic Press, p. 163.

Eisenman, G. (1962) Cation selective glass electrodes and their mode of operation. *Bioph. J.* 2:259-323.

Guidoni, L, Torre, V. and Carloni, P. (2000) Water and potassium dynamics inside the KcsA K^+ channel. *FEBS Letters* 477:37-42.

Hille, B. (1992) *Ionic Channels of Excitable Membranes* (2^{nd} Ed.) Sunderland, MA, Sinauer Assoc.

Levitt, D.G. (1999) Modeling of ion channels. *J. Gen. Physiol.* 113:789-794.

Miller, C. (1999) Ionic hopping defended. *J. Gen. Physiol.* 113:783-787.

Nonner, W., Chen, D.P., and Eisenberg, B. (1999) Perspective: progress and prospects in permeation. *J. Gen. Physiol.* 113:778-782.

Roux, B. and MacKinnon, R. (1999) The cavity and pore helices in the KcsA K^+ channel: Electrostatic stabilization of monovalent cations. *Science* 285:100-102.

Yellen, G. (1999) The bacterial K^+ channel structure and its implications for neuronal channels. *Curr. Opin. in Neurobiol.* 9:267-273.